Pakistan Veterinary Journal

ISSN: 0253-8318 (PRINT), 2074-7764 (ONLINE)
DOI: 10.29261/pakvetj/2025.323

RESEARCH ARTICLE

Protective Role of Lotus Leaf Polysaccharides in Mice with Ulcerative Colitis

Wenying Bi [1, #], Jitao Sun [2, #], Ying Zhang [1, #], Zhaojing Luo [4, #], Xue Zhang [6], Na Xia [1], Baoying Chen [1], Yanyun Che [7, 8], Sandie Siew Shean Choong [5], Liwei Guo [4, 8], Weijie Qu [1], Xiaonan Yang [9], Yi Wu [3, 8, *], Xin Wu [1, *] and Qiu Zhong [3, *]

[1]College of Veterinary Medicine, Yunnan Agricultural University, Kunming, China; [2]College of Basic Medicine, Inner Mongolia Medical University, Hohhot, China; [3]Guangxi Key Laboratory of Animal Breeding, Disease Control and Prevention, College of Animal Science and Veterinary Medicine, Guangxi University, Nanning, Guangxi, China; [4]School of Animal Science, Yangtze University, Jingzhou, China; [5]Faculty of Veterinary Medicine, Universiti Malaysia Kelantan, Kota Bharu, Malaysia; [6]College of Animal Science and Technology, Yunnan Agricultural University, Kunming, China; [7]China Engineering research center for homology of medicine and food beverage of Yunnan Province, College of Pharmaceutical Science, Yunnan University of Chinese Medicine, Kunming, China; [8]Yunnan Characteristic Plant Extraction Laboratory, Kunming, China; [9]National Engineering Research Center for Southwest Endangered Medicinal Resources Development, Guangxi Botanical Garden of Medicinal Plants, Nanning 530023, China.
#These authors contributed equally to this work.
*Corresponding author: wuyi2001cn@163.com (YW); wuxinddl@hotmail.com (XW); zhongqiujob@163.com (QZ)

ARTICLE HISTORY (25-876)

Received: September 10, 2025
Revised: November 19, 2025
Accepted: November 25, 2025
Published online: December 23, 2025

Key words:
Lotus leaf polysaccharide
RAW264.7
Ulcerative colitis
Intestinal barrier
Intestinal flora.

ABSTRACT

The incidence of ulcerative colitis (UC) is increasing worldwide, and the development of drugs to protect against UC is imminent. Lotus leaf polysaccharides (LLP) have anti-inflammatory effects. It is necessary to investigate whether they are effective against ulcerative colitis. This study aimed to evaluate the anti-UC effects. RAW264.7 LPS-induced inflammation model and a Dextran Sulfate Sodium Salt (DSS)-induced ulcerative colitis model in mice were used to assess the anti-UC effects of LLP. LLP can improve the antioxidant activity and anti-inflammatory effects in the LPS-induced RAW264.7 inflammation model. In the DSS model, LLP significantly improved pathological features, including increased body weight, colon length, reduced bloody stool, and effective protection of the intestinal structure, as well as inhibition of inflammatory factor production. LLP also increased the goblet cell numbers (as determined by PAS staining), significantly enhanced the tight junction (TJ) protein (Claudin-1, Occludin, ZO-1) expression ($P<0.05$), which helps maintain the integrity of the intestinal barrier, and inhibited the TLR4-MAPK/NF-κB signaling pathway. Furthermore, analysis of colon microbiota in DSS-treated mice revealed that LLP restored the bacterial structure damaged by DSS, improved the composition of intestinal flora, and increased the ratio of the *Firmicutes/Bacteroidetes* ratio. Additionally, metabolite analysis showed that LLP altered metabolite profiles and up-regulated pathways involving arginine, ornithine, and lysine, which may be associated with LLP's inhibition of UC. Overall, LLP exerts anti-UC effects by modulating gut microbiota and metabolism, enhancing antioxidant capacity, and strengthening the integrity of colonic tight junctions.

To Cite This Article: Bi W, Sun J, Zhang Y, Luo Z, Zhang Z, Xia N, Chen B, Che Y, Choong SSS, Guo L, Qu W, Yang X, Wu Y, Wu X and Zhong Q, 2025. Protective role of lotus leaf polysaccharides in mice with ulcerative colitis. Pak Vet J. http://dx.doi.org/10.29261/pakvetj/2025.323

INTRODUCTION

This study was performed to investigate the protective effects of lotus leaf polysaccharide contents (LLP) against ulcerative colitis (UC) and the underlying mechanisms, with a focus on their regulation of gut microbiota and metabolism. While LLP have demonstrated promising antioxidant and immunomodulatory properties, their role in the treatment and prevention of UC remains unclear.

UC, a major type of inflammatory bowel disease (IBD), manifests as mucosal inflammation and damage of intestinal walls, associated with diarrhea, abdominal pain, and bloody stools (Alhobayb and Ciorba, 2023). It is often triggered by barrier damage, immune dysregulation, and gut microbiota disorders (Zhang *et al.*, 2022)(Qin *et al.* 2023). This widespread condition is particularly severe in developing countries, frequently leading to complications and an increased risk of colon cancer (Quaresma *et al.*,

2022) (Eisenstein, 2018). Current treatments, such as 5-Aminosalicylic acid (5-ASA), have limited effectiveness and can cause serious adverse effects, making developing more effective and well-tolerated therapies an urgent priority (Gurtner *et al.*, 2023).

Natural plant polysaccharides treat UC by enhancing intestinal microecology and immunity and regulating metabolism (Wei *et al.*, 2024). They act through microbiota-dependent and -independent mechanisms (Cai *et al.*, 2020). Digestible polysaccharides modulate immunity directly, while indigestible ones shape the gut microbiota (Dilixiati *et al.*, 2024; Tan *et al.*, 2024). Thus, plant polysaccharides are an effective strategy for UC by impacting gastrointestinal bacteria and metabolites.

Nelumbo nucifera Gaertn, is a plant of nutritional and medicinal importance belonging to the Lonicera family, commonly found in China (Deng *et al.*, 2023). Meridian tropism predominantly manifests in the stomach, spleen, and liver, meridians. Within the Chinese Traditional Medicine framework, it is incorporated into numerous therapeutic formulations targeting a spectrum of conditions, such as summer heat-induced wasting-thirst, diarrhea resulting from summer heat-dampness, hematochezia, and reduced spleen, as well as spotting and flooding (Zheng *et al.*, 2022). Lotus leaves are rich in alkaloids, flavonoids, and polysaccharides, which are crucial bioactive constituents. Nuciferine, a key alkaloid in lotus leaves, exhibits anti-inflammatory, anti-obesity, and lipid-lowering effects. Flavonoids from lotus leaves are characterized by their antioxidant properties and ability to regulate the microbiota of the gut (Feng *et al.*, 2023; Ma *et al.*, 2023). Additionally, LLP possess immunomodulatory activities (Liu *et al.*, 2024; Su *et al.*, 2024), but their protective mechanisms in UC remain to be elucidated.

To address this gap, the present study systematically evaluated the anti-UC efficacy of LLP using an LPS-induced RAW264.7 macrophage model and a dextran sulfate sodium (DSS)-induced mouse model of colitis. By integrating analyses of intestinal barrier integrity, inflammatory responses, gut microbiota composition, and metabolomic alterations, this research provides a comprehensive understanding of LLP's bioactivity and offers theoretical support for developing LLP-based interventions against UC.

MATERIALS AND METHODS

Animals and cell lines: Male C57/BL6 SPF mice (5 weeks, 18-22 g) from Yangzhou University were housed under standard conditions (22 ± 1°C, 50 ± 1% relative humidity, and a 12-hour light/dark). The study was approved by the Nanjing Agricultural University Ethics Committee (SYXK (Su) 2022-0026, Nov 27, 2022).

The RAW264.7 cell lines were taken from National Center for Cell Culture Resources (Chinese Academy of Sciences) and then cultured in DMEM (high glucose, Biological Industries) and supplementation of 10% FBS (Gibco) was done at temperature of 37°C in 5% CO_2 concentration.

Extraction of LLP: Crude lotus leaf polysaccharides (LLP) were prepared using a modified water–ethanol extraction method(Wu *et al.* 2024). Dried lotus leaves 350 g were first refluxed three times with 3 L of 70% ethanol at 80°C for time of 2 h each to remove pigments, alkaloids, and lipophilic compounds, yielding a defatted residue. The residue was then extracted three times with pure water (10 × volume) at 70°C for 2 h each. The combined aqueous extracts were filtered and concentrated under reduced pressure to approximately one-tenth of the initial volume.

To precipitate polysaccharides, 95% ethanol was added to the concentrated extract to reach a final ethanol concentration of 80% (v/v), followed by overnight precipitation at 4°C. The precipitate was collected by centrifugation at 1500 rpm for 10 min, washed sequentially with ethanol and acetone, and vacuum-dried at 45°C to obtain the crude polysaccharide fraction.

The crude LLP was dissolved at a concentration of 10 mg/mL in deionized water and deproteinized using the Sevag method (chloroform:n-butanol = 4:1, v/v) five times. The solution was then dialyzed against distilled water (molecular weight cut-off = 3.5 kDa) for 72 h to remove small molecules, followed by freezing at -80°C for 8 h and lyophilization for 72 h to obtain deproteinized crude LLP. The yield was 11.93 g (3.41%), and the freeze-dried powder was stored at temperature of -20°C.

Construction of in vivo and in vitro UC models: After 1 week of acclimation, groups received: Control (normal water/diet) or DSS (3% in water, days 0-7). Converted according to the human equivalent dose, it is considered a medium dose. Twice the medium dose is considered a high dose. Half the medium dose is considered a low dose. During the experiment, mice in the Control group had free access to water daily, while mice in the Model group consumed water containing 3% DSS daily. In addition to receiving water containing 3% DSS daily, mice in the treatment group were administered LLP at different concentrations via gavage. Treatment groups also received LLP by gavage: LLP-L (50 mg/kg), LLP-M (100 mg/kg), or LLP-H (200 mg/kg). On day 8, mice were euthanized; colon length was measured, spleen/thymus weighed for organ index, and tissues/blood collected for analysis (Fig. 2A).

RAW264.7 cells were stimulated with LPS to model UC and treated with LLP (100-1000 μg/mL). Supernatant levels of SOD, CAT, GSH, LDH, NO, TNF-α, IL-6, IL-8, and IL-10 were measured (Lianke Biotech kits).

Evaluation of the effect of drug therapy in vivo: During modeling, daily body weight and bloody stool were recorded to calculate the Disease Activity Index (DAI) (Zioga *et al.*, 2022). Scores are shown in Table 1.

Table 1: Disease activity index（DAI）score criteria of mice

Weight loss1%	Fecal character	Blood with fecal	Score
＜1	Shape and hard	None	0
1-5	Formed but fluffy and invisible	Blood with fecal	1
5-10	Not rigorous	A little blooding is visible.	2
10-15	Mild diarrhea	Amount of blooding visible	3
＞15	Severe diarrhea	Visible rectal bleeding	4

Hematoxylin and Eosin (H&E) and Periodic acid Schiff's (PAS) Staining: Colon tissues (about 1 cm^3) were

fixed, dehydrated, transparent, and embedded in dipping wax, then cut into thin slices and pasted on slides, and finally stained with H&E (G1121, Solabo, China) and PAS. Tissue morphology was observed microscopically.

Immunofluorescence (IF) analysis: Colon tissue preparation was done as per description insection 2.5. Staining was performed as described in Ruan et al (Ruan *et al.*, 2024). Sections were incubated with E-Cadherin antibody (1:500, P12830, Merck, Germany) and Anti-Occludin antibody (1:500, Q16625, Merck, Germany) for 1 h at room temperature, followed by DAPI (MBD0015, Merck, Germany) staining.

Western blot (WB): Colon tissue proteins were extracted using RIPA buffer (Solabo). Samples were denatured, separated by SDS-PAGE, and transferred to PVDF membranes. Membranes were blocked (5% BSA, 2h), incubated with primary/secondary antibodies, and developed using chemiluminescence (GE Amersham). Detailed antibody information is presented in Table 2.

Table 2: Detailed antibody information.

Antibody	Host	Dilution
TLR4	Rabbit	1:1000
ERK	Rabbit	1:1,000
p-ERK	Rabbit	1:1,000
p-38	Rabbit	1:1,500
p- p38	Rabbit	1:2,000
p-65	Rabbit	1:1,500
p- p65	Rabbit	1:2,000
a-tubulin	Rabbit	1:1,500
GAPDH	Rabbit	1:2,500
Goat Anti-Rabbit IgG H&L (HRP)	Goat	1:8,000

Gut Microbiota Sequencing: Mouse intestinal flora was analyzed through high-throughput sequencing of the V3-V4 variable region (Shanghai, China). Fecal DNA was extracted and subjected to PCR amplification, followed by purification, elution, and library construction for sequencing by Parsons Brinckerhoff.

Metabolomic analysis: Metabolites from colon contents (20 mg) were extracted using methanol-water with internal standard (Thermo Fisher). LC-MS data was processed (Progenesis QI), features matched against HMDB/Metlin databases. Statistical analyses (PCA, OPLS-DA) identified differential metabolites (VIP>1, P<0.05) (Yi *et al.*, 2016).

Statistical Analysis: Statistical outcomes are presented in mean±standard deviation. Analysis of Data was conducted using SPSS 21.0 and GraphPad Prism 10.4. Assessment of normality of Data was assessed was done using Shapiro–Wilk tests, while variance homogeneity was analyzed via Levene's test. For multi-group comparisons, one-way ANOVA was applied, followed by Bonferroni-adjusted Student's t-tests when significant differences were detected. The level of significance was assumed at 95% confidence interval (P<0.05).

For 16S rRNA metabolomics and sequencing datasets, analyses were done in the R 4.4.0 environment using appropriate bioinformatics packages. Differential microbial taxa and metabolite profiles were evaluated with non-parametric statistical tests based on data characteristics. Multiple testing corrections were implemented using the Benjamini–Hochberg procedure to control the false discovery rate. Features exhibiting $|\log_2$ fold change$| > 1$, along with statistical significance, were defined as biologically meaningful differences.

RESULTS

Antioxidant and anti-inflammatory effects of LLP in vitro: To assess the anti-inflammatory and antioxidant effects of LLP in vitro, we used RAW264.7 cells to establish a UC model by LPS. The in vitro antioxidant results of LLP showed that Both LLP samples showed strong DPPH free radical scavenging (84.94%) (Fig. 1A) and ABTS scavenging (96.96%) (Fig. 1B) at a concentration of 10,000 μg/mL. T-AOC tests indicated a total antioxidant capacity of 2.91 mM at the same LLP concentration (Fig. 1C). The safe concentration of LLP was determined by CCK-8. The results showed that LLP had no effect on cell viability when its concentration was less than 200 μg/mL (P≥0.05) (Fig. 1D). Following LPS treatment, LDH activity, CAT activity, and NO release decreased in a dose-dependent manner with increasing LLP concentration. At 200 μg/mL of LLP, LDH activity was 272.3 U/L (P<0.0001) (Fig. 1F), CAT activity was 3.78 U/mg (P<0.0001) (Fig. 1G), and NO release was 7.23 μM/mL (P<0.0001) (Fig. 1I). SOD activity and GSH levels increased in dose dependent fashion. In comparison to the LPS, at 200 μg/mL of LLP, SOD activity was 22.74 U/mL (P<0.001) (Fig. 1E), and GSH content significantly rose to 3.39 μm/gprot (P<0.05) (Fig. 1H). After LPS stimulation, RAW264.7 cells released large amounts of IL-6, TNF-α, IL-10, and IL-1β, and their levels decreased as LLP concentration increased. At 200 μg/mL of LLP, the levels of IL-10, TNF-α, and IL-1β, were 511.80 (P<0.05), 1889.5 (*P*<0.001), 1276 (P<0.0001), and 246.8 (P<0.0001) pg/mL, respectively (Fig.s 1J-M). These findings suggest that LLP at 200 μg/mL exhibits significant anti-inflammatory and antioxidant effects in vitro.

LLP ameliorates DSS-induced UC symptoms: To further explore the in vivo effects of LLP on UC, the body mass and DAI score of the mice were monitored and recorded. Intestinal injury occurred in mice after DSS ingestion, as evidenced by weight loss, diarrhea, and the presence of mucoid or bloody stools (Fig.s 2B-D). In comparison to the DSS group, the LLP-H group had slower weight loss. Comparing with the DSS group, the DAI value and LLP concentration showed a dose reduction, and the DAI value decreased significantly with the increase of polysaccharide concentration after the intervention in the LLP group (P<0.05) (Fig. 2D). DSS affected colon length (Fig.s 2C, E) in mice. the colon tissue of the Con group was intact after H&E staining. The intestinal epithelial cells were tightly connected with the muscular layer, and the crypts were intact. In DSS group, the colon tissue was severely damaged and neutrophil infiltration was absent. Compared with the DSS group, the DSS group had severe colon tissue damage, shedding of intestinal epithelial cells, disappearance of crypts, and more severe neutrophil infiltration. Crypt damage was attenuated, and neutrophil infiltration was reduced in LLP-M and H groups. The results of PAS staining showed that the number of goblet cells in the DSS group was significantly reduced, and the

mucosal layer was damaged, thinner or even disappeared. After LLP intervention, the number of goblet cells increased with the increase of LLP concentration, and the mucosal layer gradually thickened. LLP effectively attenuated DSS-induced experimental colitis and improved gut structure (Fig. 2F).

LLP regulates NO and pro-inflammatory cytokine production: Cytokine levels were measured in serum (Fig. 3A-E) and colon tissue (Fig .s 3F-J) of each group of mice. The levels of NO (Fig. 3A), TNF-α (Fig. 3B), IL-6 and IL-1β in the serum of mice in the DSS group were significantly increased (P<0.01) (Fig. 3C, D), while the level of IL-10 (Fig. 3E) was significantly decreased (P<0.01). Comparing to DSS group, LLP-H significantly reduced the levels of NO, TNF-α, IL-6 and IL-10 in serum, reduced the levels of NO, IL-6, IL-1β and IL-10 in colon (P<0.01), and significantly reduced the level of TNF-α in colon (P<0.05). It also significantly increased IL-10 levels in serum and colon (P<0.01). These results indicate that LLP can reduce the levels of pro-inflammatory factors and increase the levels of anti-inflammatory factors in colon tissue. Compared with the serum group, the effect was more obvious.

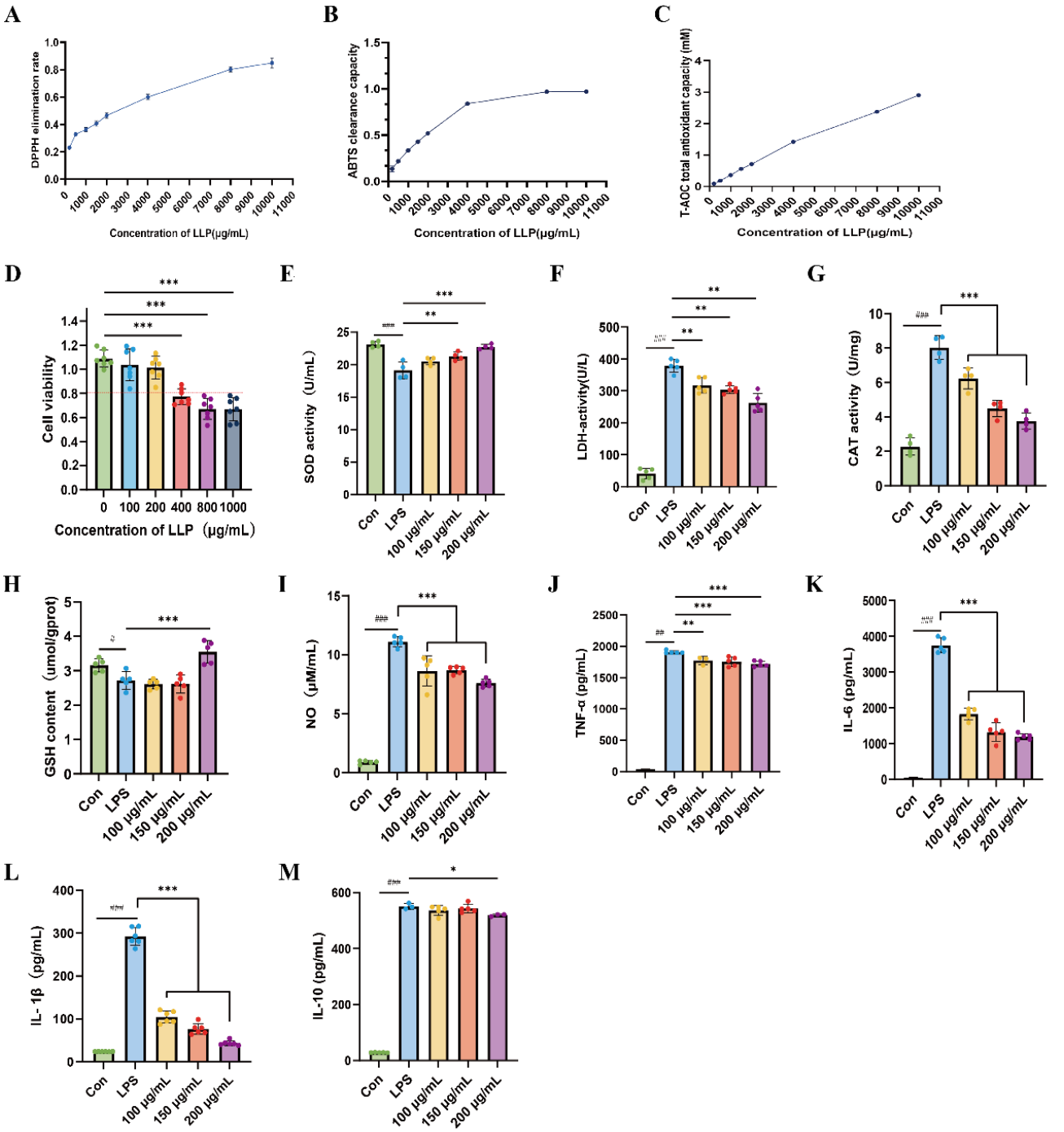

Fig 1: LLP with in vitro antioxidant and anti-inflammatory activity. (A) DPPH scavenging, (B) ABTS scavenging capacity, (C) T-AOC total antioxidant capacity of LLP. (D) Determination of RAW264.7 cell viability of LLP. (E-H) Effect of LLP on RAW264.7 antioxidant factors LDH (E), CAT (F), SOD (G), GSH (H). (I-M) Cytokine expression of RAW264.7 on NO (I), TNF-α (J), IL-6 (K), IL-1β (L), IL-10 (M) by LLP. Note: ns indicates P>0.05, no significant difference, * indicates P<0.05, ** indicates P<0.01, *** indicates P<0.001, significant difference with the DSS group.

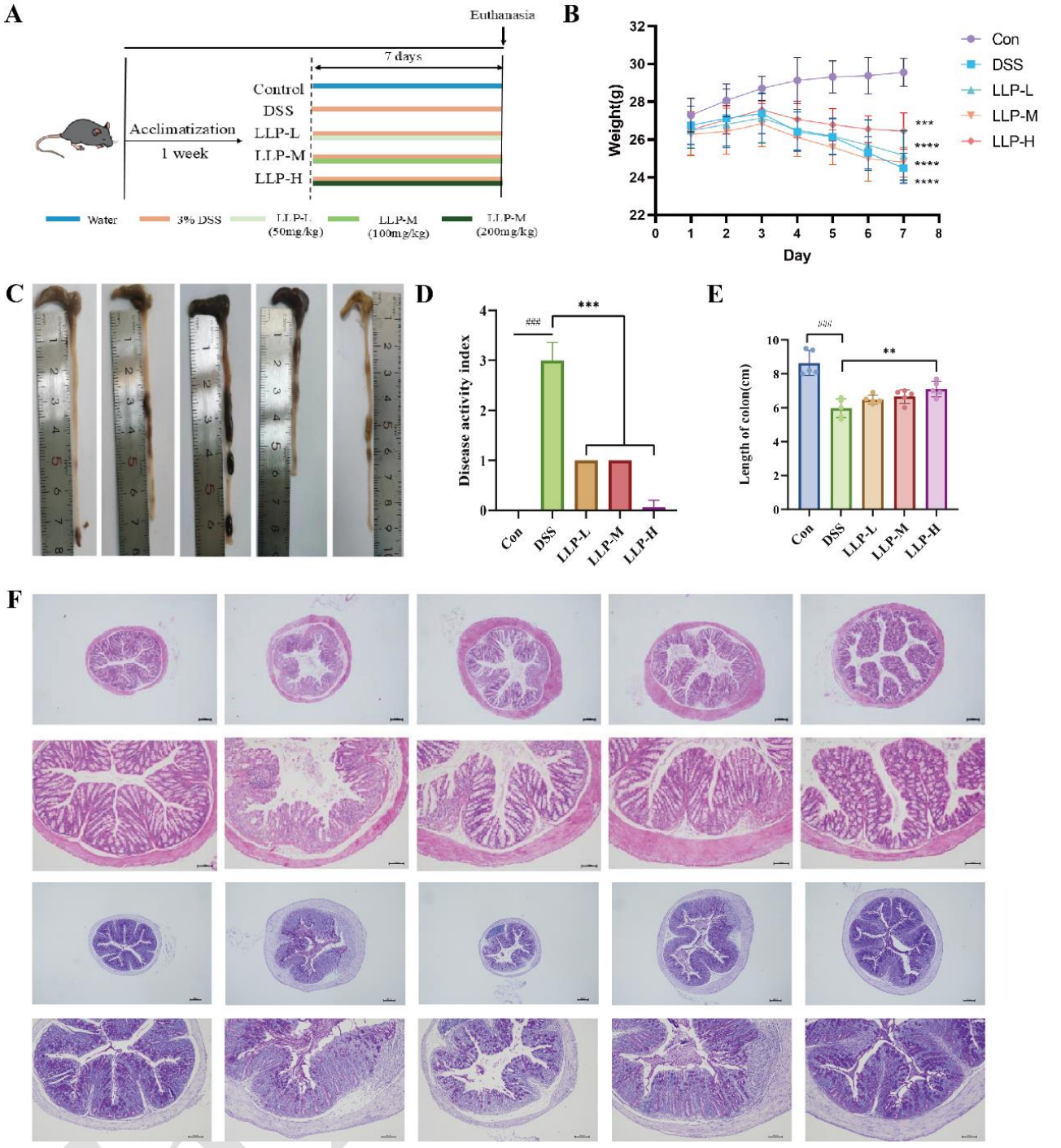

Fig 2: Effect of LLP on symptoms and histopathologic changes in ulcerative colitis (UC). (A) Animal experimentation pattern diagram. (B) Mouse body weight curve. (C) Representative images of the colon in each experimental group. (D) Mouse DAI change scores. (E) Length of colon. (F) Histopathologic staining of sections of the distal colon (H&E,40×, 100×) (up), Mouse colon PAS staining (40×, 100×) (down). Note: ns indicates P>0.05, no significant difference; * indicates P<0.05, ** indicates P<0.01, *** indicates P<0.001, significant difference with the DSS group.

LLP reduced inflammation through the TLR4-MAPK/NF-κB pathway: Given the evidence that LLP ameliorates inflammation, we selected the TLR4-MAPK/NF-κB pathway, a canonical inflammatory cascade, for further validation. The expressions of TLR4, NF-κB and MAPK signaling pathway-related proteins in the colon tissues of Con, DSS and LLP-H groups were detected by WB (Fig. 4A). The results showed that DSS increased TLR4 proteolysis in the mouse colon. In the LLP group, the level of TLR4 decreased compared with that in the DSS group, indicating that LLP could inhibit the activation of the TLR4 pathway (P<0.01) (Fig.s 4A-B). DSS increased the levels of MAPK proteins p-p38, p-ERK in the mouse colon. However, in the LLP-H group, each phosphorylation was inhibited to different degrees, and p-p38/p38p-ERK/ERK (P<0.05 or P<0.01) (Fig.s 4A, C-D) were reduced compared to the DSS group, respectively, suggesting that Lotus leaf polysaccharides inhibit the activation of the MAPK pathway. DSS increased the level of p-p65 in the mouse colon. However, in the LLP-H group, its phosphorylation was inhibited and p-p65/p65 was reduced compared to the DSS group (P<0.05) (Fig.s 4A&E). Illustrated that LLP-H was found to inhibit the TLR4-MAPK/NF-κB signaling pathways activation.

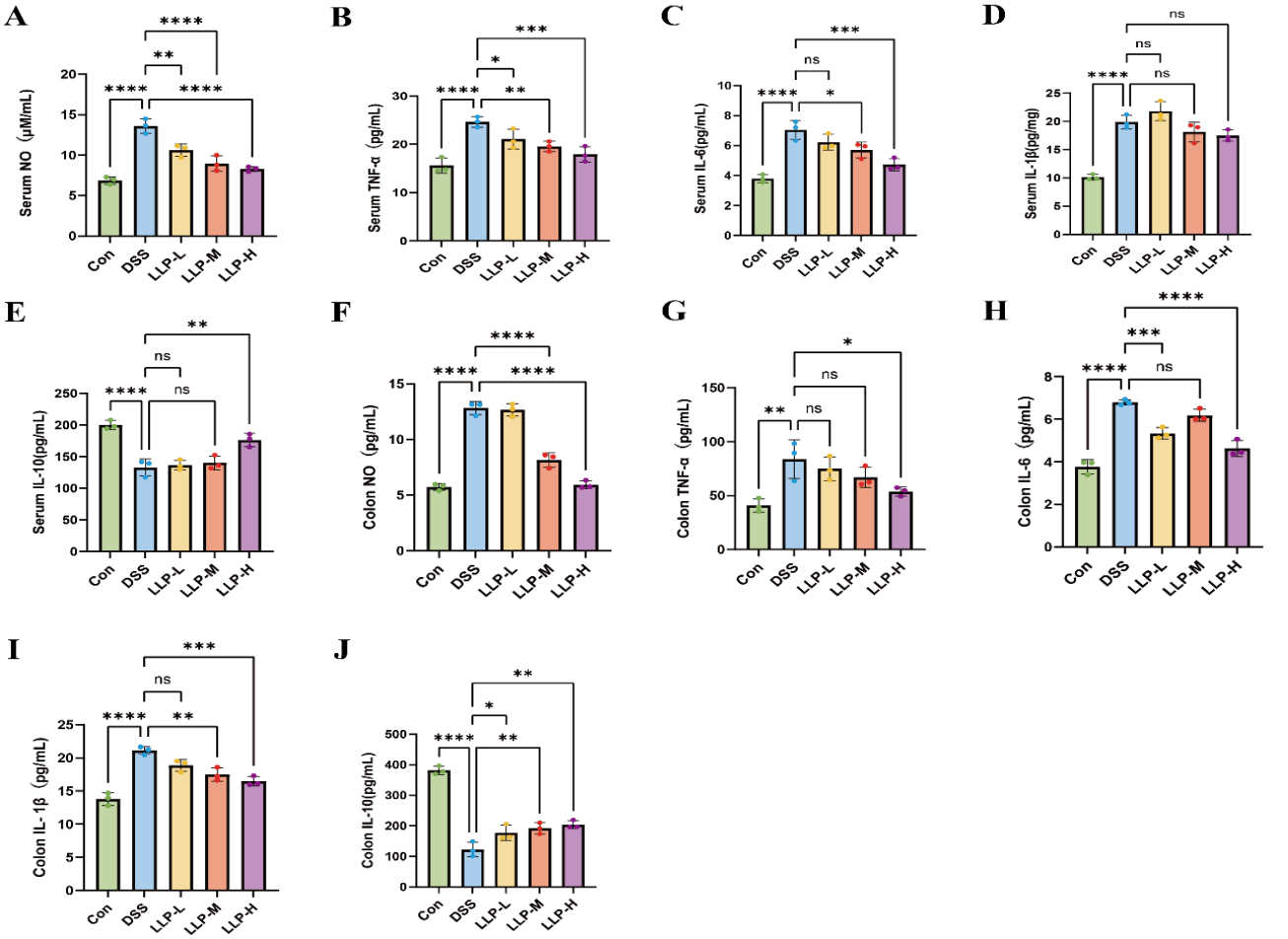

Fig 3: Effect of LLP on the release of inflammatory factors in mice. Serum NO (A), TNF-α (B), IL-6 (C), IL-1β (D), and IL-10 (E). Colonic tissue NO (F), TNF-α (G), IL-6 (H), IL-1β (I), IL-10 (J). Note: ns indicates P>0.05, no significant difference, * indicates P<0.05, ** indicates P<0.01, *** indicates P<0.001, significant difference with the DSS group.

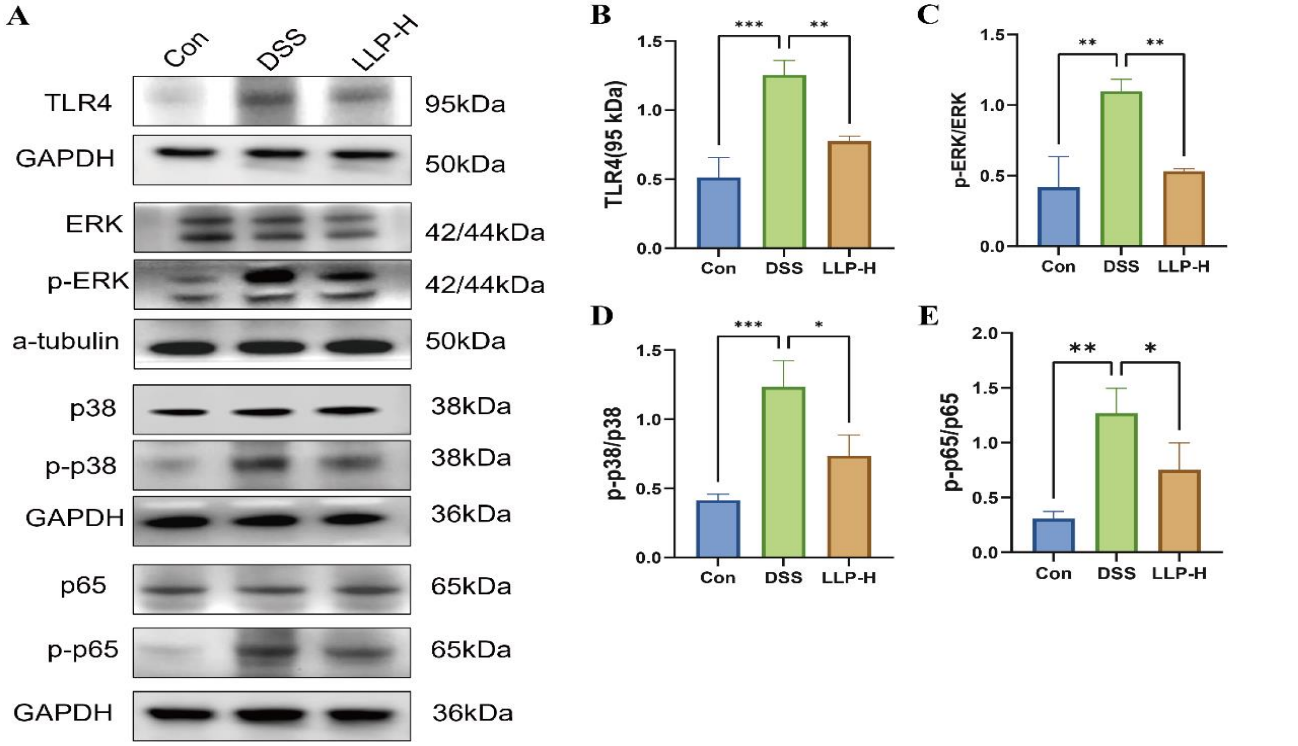

Fig 4: LLP can inhibit the TLR4-MAPK/NF-κB pathway. (A)Protein blot, (B) TLR4relative protein content, (C) p-ERK/ERKrelative protein content, (D)p38/p-p38relative protein content, (E)p-p65/p65relative protein content. Note: ns indicates P>0.05, no significant difference, * indicates P<0.05, ** indicates P<0.01, *** indicates P<0.001, significant difference with the DSS group.

LLP altered the diversity and structure of intestinal microflora in UC mice: For the determination of effects of LLP associated with alterations in the gut microbiota of UC mice, the researchers performed 16S rRNA sequencing. Principal component analysis revealed that the LLP treatment group was close in distance, indicating a similar gut microbial structure, close to the Con group, and that DSS significantly disrupted normal gut flora (Fig. 5A). It means that LLP restores the normal gut flora structure that has been disrupted by DSS. Alpha diversity showed that the coverage index of all samples was more than 0.98 for all samples, showing that the sequencing data accurately reflect the changes in the intestinal flora of mice. Chao-1 & Shannon's index showed LLP-H was more diverse than the DSS group, LLP increased species diversity and richness compared to the UC mice (Fig. 5B). Results indicate that LLP can alter the structure of gut microbiota and increase the population of bacteria, mitigating DSS-induced UC microbiota structure and increasing the abundance and diversity of bacterial populations, thereby mitigating DSS-induced UC and diversity.

Species distributions of the gut microbiota were analyzed using species distribution histograms and heat maps. At the phylum level, the predominant bacteria were *Firmicutes, Actinobacteriota,* and *Dferribacterota* (Fig.s 6A-B). *Bacteroidota* abundance relative was higher than the DSS group in mice after LLP treatment. the dominant families that were identified at the family levels included *Lachnospiraceae, Oscillospiraceae,* and *Muribaculaceae* (Fig.s 6C-D). In the DSS group, *Muribaculaceae* was decreased but *Lachnospiraceae* was increased, whereas LLP treatment increased relative bacterial abundance of given families. While the major genera of bacteria detected in the samples were *Muribaculaceae*, *Lachnospiraceae_NK4A136_*group, and *Faecalibaculum* (Fig.s 6E-F). As a beneficial bacterium, low levels of *Faecalibaculum* were associated with intestinal inflammation, whereas the DSS group had the highest *Faecalibaculum*, probably due to the high bacterial value added as modeling.

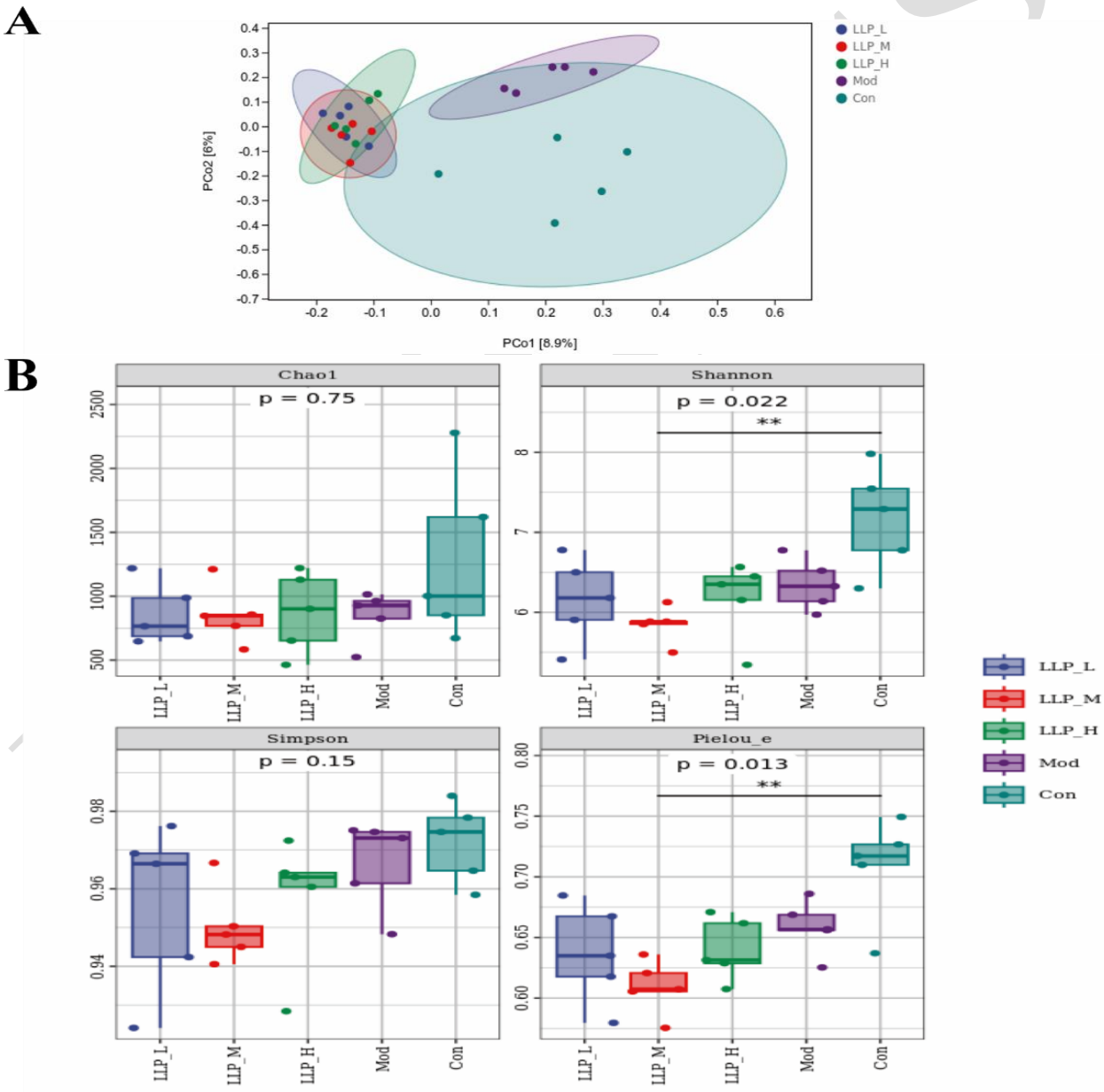

Fig 5: LLP treatment significantly altered the diversity of the gut microbiota: (A) principal coordinate analysis plot (PCoA) and (B) α-diversity box plots (Good's coverage, Chao 1, Shannon's index, and Simpson's index). Note: Values are expressed as mean ± SD, n = 5. Significant differences are expressed as* indicates P<0.05, ** indicates P<0.01, *** indicates P<0.001.

LLP regulates arginine metabolism to alleviate DSS-induced UC: Since there were large changes in gut microbiota in Con, DSS and LLP-H groups, we hypothesized whether such changes would cause changes in colonic metabolites in mice. Therefore, metabolomic assays were performed in the mouse colon. PLS-DA was performed on standardized data (Fig.s 7A-B). It was shown that the Con group was completely separated from the LLP-H and DSS groups in the positive and negative ion patterns, while the LLP group was also largely separated from the DSS group, indicating significant differences in metabolites among the three groups of mice. OPLS-DA analysis combined with t-test analysis was used to screen out the differential metabolites related to colitis (VIP>1, P<0.05) as potential biomarkers. Potential biomarkers were analyzed by volcano plot (Fig.s 7C-E), in the DSS group a total of 287 markers were down-regulated and 211 markers were up-regulated compared with the Con group, 217 markers were down-regulated and 184 markers were up-regulated in the LLP group compared with the DSS group. A total of 41 markers were down-regulated and 61 markers were up-regulated in the Con group compared with the LLP group. The results showed that after treatment it was able to alter the composition of colonic metabolites in DSS mice.

In addition, the pathways differentially associated with DSS and Con group were FcγR-mediated phagocytosis and down-regulation of ABC transporter proteins, as well as up-regulation of bile secretion (Fig. 7F). The different pathways differentially associated with LLP versus DSS mainly include the upregulation of arginine biosynthesis and metabolism of alanine, aspartic acid, and glutamate; and the promotion of biosynthesis of ornithine, lysine, and nicotinic acid-derived alkaloids. These may be related to the suppression of enteritis by LLP (Fig. 7G). These results tell us that changes in metabolites may be answerable for relocation UC. These results suggest that LLP may achieve its therapeutic effect on UC by alleviating inflammatory damage and restoring the colonic barrier.

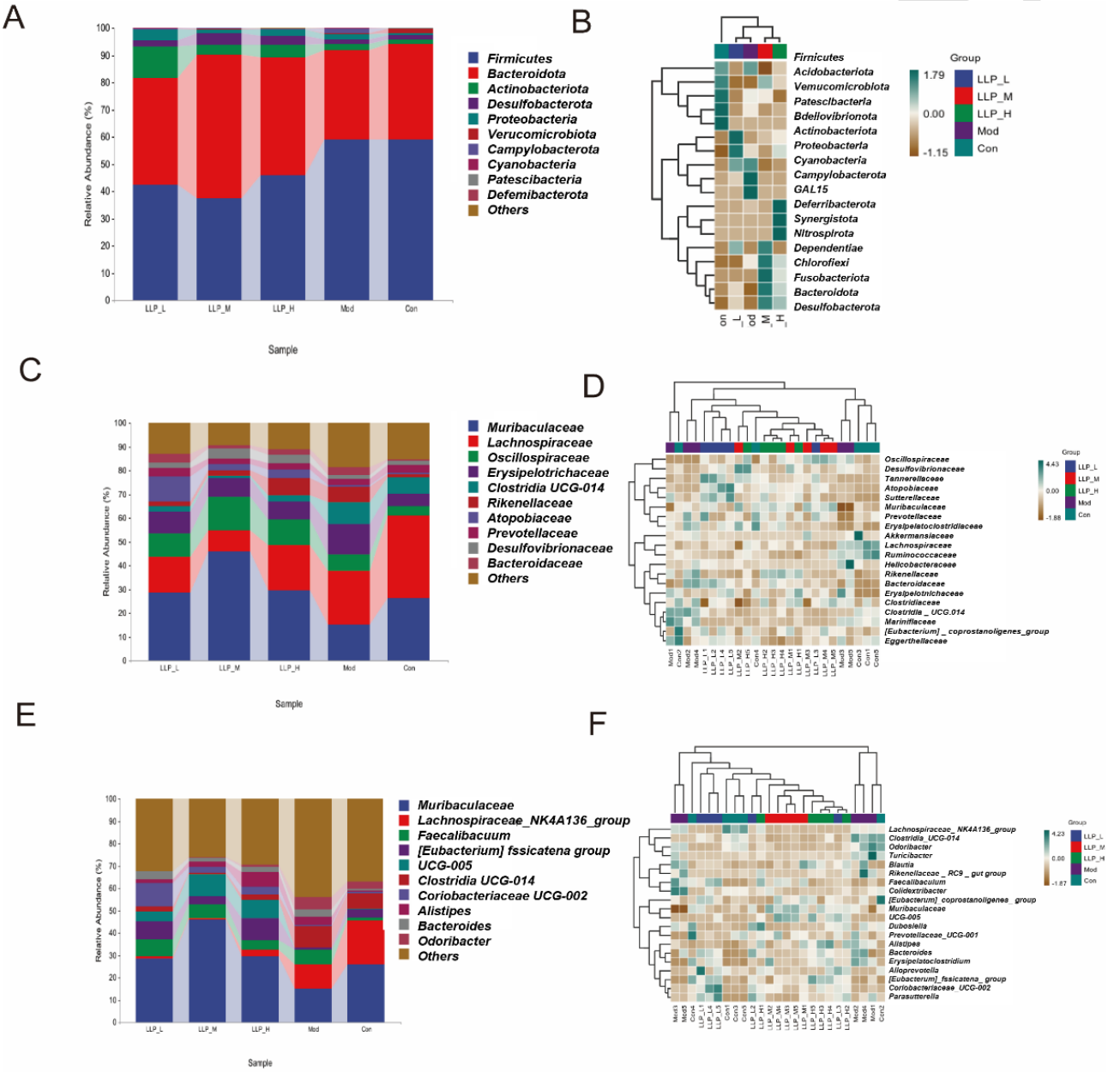

Fig 6: LLP treatment significantly altered the composition of the gut microbiota. Phylum (A) family(C), and genus (E)levels level relative abundance. Heatmap of species composition at the phylum (B), family (D), and genus (F) levels.

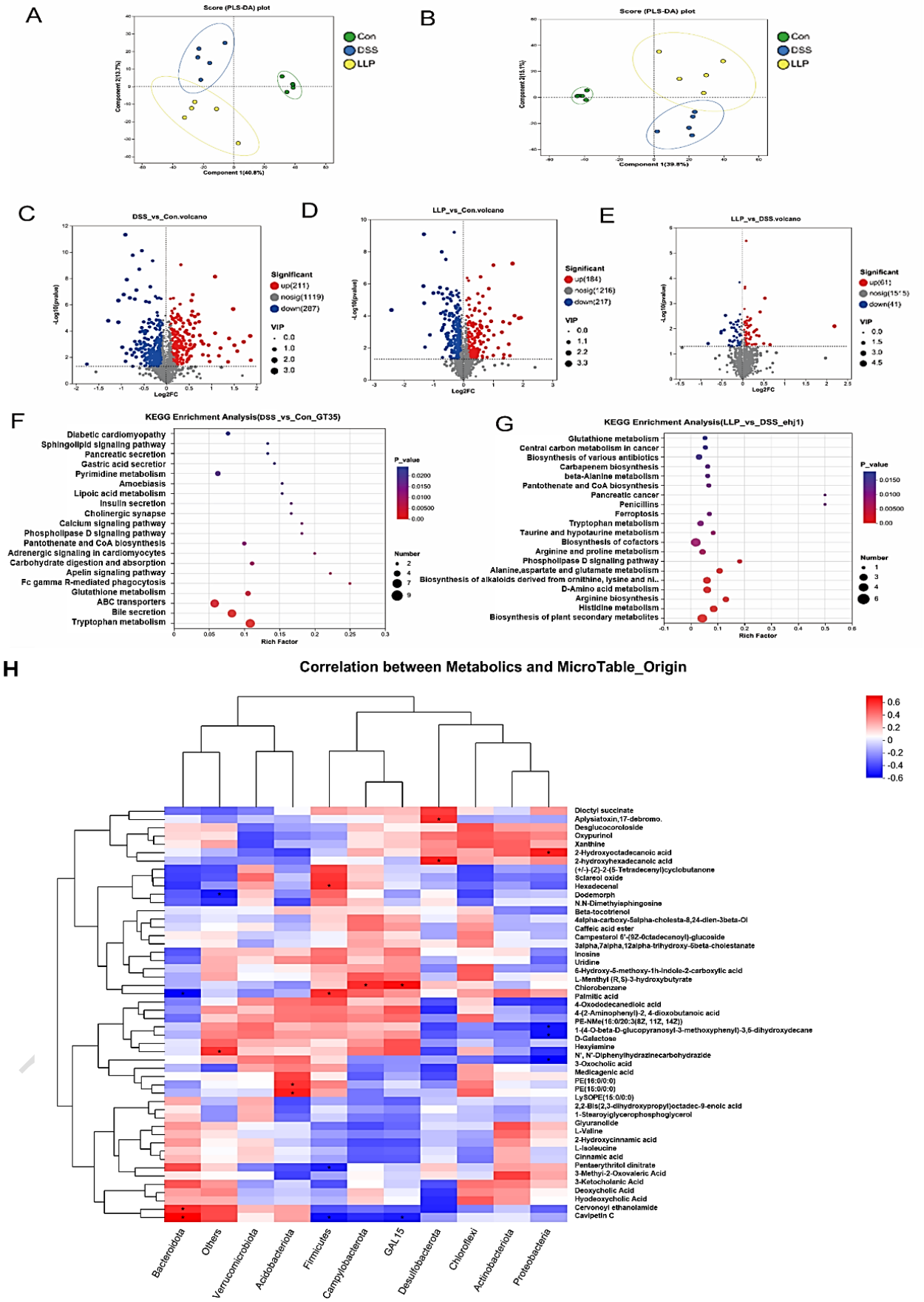

Fig 7: Fecal metabolomics for metabolite quantification in the dextran sulfate sodium (DSS) and LLP group. (A) PCA principal component analysis. (B) Venn diagram of LLP, DSS distribution group and control group. (C-E) Volcano plot showing differential accumulation and significant changes in metabolites in the LLP group compared to the dextrose sodium sulfate (DSS) group, Con group. (F-G) The metabolites were annotated into different metabolic pathways by KEGG-based enrichment bubble maps in positive and negative ion modes. (H) Analysis of the correlation between intestinal microorganisms and metabolism in mice. Different colors represent the magnitude of correlation coefficients between attributes. Note: ns indicates P>0.05, no significant difference, * indicates P<0.05, ** indicates P<0.01, *** indicates P<0.001, significant difference.

To understand the relationship between gut contents microbiome and metabolome, correlation analyses were performed. Spearman correlation analysis was performed between the changes in metabolites screened by metabolomics analysis and the differences in the genus level of intestinal flora screened by 16S rRNA gene sequencing analysis. The correlation coefficient $|r|>0.60$ and $P<0.05$ were considered as statistically significant differences. The results showed that bacteroidota increased cavipetin c and cervonoyl ethanolamide and decreased palmitic acid. *Acidobacteriota* can increase Phosphatidylethanolamine (PE) and lysophosphatidylethanolamine (lysoPE). *Firmicutes* could reduce cavipetin c, Pentaerythritol dinitrate and increase palmitic acid. *Campylobacterota* and GAL15 could increase chlorobenzene. *Desulfobacterota* increased aplysiatoxin 17-debromo and 2-hydroxyhexadecanoic acid. *Proteobacteria* can reduce 1-(4-O-beta-D-glucopyranosyl-3-methoxyphenyl)-3,5-dihydroxydecane, D-Galactose, 3-oxocholic acid, 2-hydroxyoctadecanoic was added (Fig. 7H).

Repaired the intestinal barrier: From the transcriptome data, we found that ABC transporters were downregulated by DSS. ABC transporters help intestinal cells to maintain proper ion and metabolite concentrations, thereby maintaining normal intestinal function. Therefore, in the maintenance of intestinal barrier it plays a vital role. Therefore, in order to further verify that DSS-induced intestinal barrier damage, for tight junction proteins we performed immunofluorescence assay (cluadin1, Occludin, ZO-1). The result showed that the DSS group was greatly decreased, in the content of all three kinds of tight junction proteins, it damaged the intestinal barrier of DSS group. In comparison with the DSS group, three of compact proteins in the LLP-M and LLP-L groups were not remarkably affected, while the contents of the three TJ proteins, ZO-1, Occludin and Claudin-1, in the LLP-H group were significantly elevated ($P<0.05$), suggesting that large dosages of LLP could preserve the intestinal barrier's structure and prevent inflammation from destroying intestinal compact proteins (Fig.s 8A-C).

DISCUSSION

For this investigation, we found the alternative efficacy of LLP in a DSS-induced UC mouse pattern, demonstrating its ability to modulate cytokines, inhibit inflammatory pathways, and restore gut microbiota balance. Metabolomic analysis reveals LLP's role in regulating arginine metabolism and intestinal barrier function, underscoring its potential as a novel UC treatment.

In vivo studies in UC mice demonstrated that LLP reduced inflammation and promoted the repair of the damaged intestinal mucosal barrier. At a concentration of 200 mg/mL, LLP significantly improved DSS-induced UC, exhibiting superior therapeutic effects compared to LLP-L (50 mg/mL). That underscores the capacity of plant polysaccharides in the analysis of UC. Astragalus polysaccharides (APS) have been shown to alleviate UC by restoring short-chain fatty acid (SCFAs) production and regulating Th17/Treg cell homeostasis in a microbiota-dependent manner(Zhang *et al.* 2025). This highlights the importance of gut microbiota in the therapeutic effects of plant polysaccharides. Similarly, polysaccharides from *Grifola frondosa* have demonstrated potential in oxazolone-induced UC by restoring oxidative balance and regulating intestinal flora, thereby improving the intestinal barrier and reducing inflammatory mediators (Liu *et al.* 2024). These findings underscore the role of polysaccharides as prebiotics that can modulate the gut microbiome to exert their therapeutic effects. The anti-inflammatory properties of polysaccharides are further exemplified by selenium-containing tea polysaccharides, which ameliorate DSS-induced UC by enhancing the intestinal barrier and regulating the gut microbiota(Zhao *et al.* 2022). By inhibiting the NF-κB pathway, almond polysaccharides also exhibit significant anti-inflammatory activity, thereby protecting against colonic tissue damage and reducing the expression of pro-inflammatory cytokines. (Peng *et al.* 2024). These studies collectively demonstrate that plant polysaccharides can effectively modulate inflammatory pathways, contributing to their therapeutic potential in UC.

Importantly, these preclinical results offer a powerful mechanistic foundation for the potential clinical translation of LLP in UC management. Meanwhile, Polysaccharides' immunomodulatory effects are linked to TLRs, particularly TLR4(Chen *et al.*, 2022). We discovered that LLP inhibits the TLR4-MAPK/NF-κB pathway, contrasting with Astragalus polysaccharides activates of TLR4 and MAPK pathways in the intestine.

Through the metabolomics data, we found that its LLP treatment of UC mainly through two pathways. One is arginine metabolism, and the other is ABC transporters. Arginine is known to play an important role to induce the immune response and gut health(Fan and Pedersen, 2021). The upregulation of arginine biosynthesis and metabolism of related amino acids, such as alanine, aspartic acid, and glutamate, observed in the LLP-treated group, indicates a possible modulation of the gut's immune response and mucosal integrity. This is in line with the known functions of arginine in promoting wound healing and maintaining the intestinal barrier. Furthermore, the promotion of biosynthesis of ornithine, lysine, and nicotinic acid-derived alkaloids in the LLP group suggests an enhancement of the gut's defense mechanisms against inflammation(Lin *et al.*, 2012). The relationship between ABC transporters and the intestinal mucosal barrier is of significant importance in maintaining gut homeostasis and health.

The correlation analysis between gut microbiome and metabolome further supports the interaction between microbial populations and metabolic pathways (Xu *et al.*, 2023). The observed changes in *bacteroidota*, *acidobacteriota*, and *firmicutes* in response to LLP treatment, and their association with specific metabolites, suggest a complex microbial-metabolite network that contributes to the amelioration of UC symptoms. For instance, the increase in *bacteroidota* was correlated with an increase in *cavipetinc* and *cervonoyl ethanolamide*, which are known to have anti-inflammatory properties, and a decrease in palmitic acid, which is associated with inflammation (Ma *et al.*, 2024). Our study observed that DSS downregulated ABC transporters, which could lead to compromised intestinal barrier function, as these

transporters are vital for maintaining proper ion and metabolite concentrations across the intestinal cells. The downregulation of ABC transporters could result in enhanced intestinal mucosa permeability, allowing for the translocation of endotoxins and bacteria into the systemic circulation, which is a hallmark of inflammatory bowel diseases like UC (Rees *et al.*, 2009). The immunofluorescence assay results indicated that the intestinal barrier in the DSS group was significantly damaged, as evidenced by the decreased statement of tight junction proteins such as claudin1, Occludin, and ZO-1. LLP's ability to restore the expression of these tight junction proteins suggests a mechanism by which it can protect and repair the intestinal barrier. By upregulating ABC transporters, LLP may enhance the efflux of pro-inflammatory substances and support the maintenance of intestinal epithelial integrity, thereby mitigating the inflammation associated with UC. Such broad-spectrum modulation suggests that LLP could serve as a complementary or adjunct therapy alongside conventional drugs like 5-ASA or corticosteroids, potentially reducing their dosage and adverse effects.

Given its natural origin, favorable safety profile, and dual regulation of gut microbiota and host metabolism, LLP could be further developed into a functional food, nutraceutical, or oral biotherapeutic formulation for UC prevention and long-term management. Future translational studies should therefore focus on pharmacokinetics, safety evaluation, and clinical dose optimization to bridge the gap from preclinical efficacy to human application. Together, these findings highlight LLP as a promising candidate for the development of novel, microbiota-targeted interventions for ulcerative colitis.

This study acknowledges its limitations. Although LLP shows promise as a therapy for DSS-induced UC, its efficacy in other colitis models remains unclear. These models include: 2,4,6-trinitrobenzenesulfonic acid-induced colitis and oxazolone-induced colitis. Furthermore, current LLP treatment is limited to the molecular level of polysaccharides. Integrating it with drug delivery systems in the future could achieve more efficient and precise therapeutic outcomes(Sun *et al.* 2024). Due to its context-dependent bioactivities, more foundational data are required. Subsequent studies should employ diverse models covering various etiologies—bacterial, parasitic, and viral—to fully evaluate LLP's protective effects against enterocolitis. Potential mechanisms could be explored using multi-omics analyses, like proteomics, transcriptomics, network pharmacology, and molecular docking. Additionally, short-chain fatty acid (SCFAs) levels should be assessed to clarify their role in LLP-mediated amelioration of UC.

Current research has confirmed that patients with IBD exhibit reduced butyrate-synthesizing genes in their microbiota and impaired receptor expression (Mukhopadhya and Louis 2025). Therefore, further investigation into the regulation of SCFAs in ulcerative colitis holds significant promise.

The absorption and structure-activity relationships of polysaccharides as biomacromolecular drugs remain poorly understood, presenting a significant challenge for us. Future research efforts should focus on elucidating the structure-activity relationships of polysaccharides.

Conclusions: The results showed that LLP effectively ameliorates DSS-induced UC by regulating the gut microbiota, modulating the metabolome, and inhibiting inflammatory pathways. Its therapeutic potential is further supported by its ability to repair the intestinal barrier for UC treatment.

Funding: This study was financially supported by the National Natural Science Foundation of China (NSFC, Grant No. 32172900 and 32560872), Guangxi Natural Science Foundation Program (Grant No. 2023GXNSFBA026354), the Open Research Fund of Yunnan Characteristic Plant Extraction Laboratory and National Natural Science Foundation of China (YKKF2024009) and Yunnan Joint International R&D Center of Veterinary Public Health (202403AP140033).

Author's contribution: Wenying Bi, Jitao Sun, Ying Zhang and Zhaojing Luo: Methodology, Investigation, Data collecting, Writing – original draft, Writing – review & editing. Xue Zhang, Na Xia and Baoying Chen: Data curation, Software, Formal Analysis, Validation, Yanyun Che, Qiu Zhong, Xiaonan Yang and Sandie Siew Shean Choong: Writing – review & editing. Weijie Qu and Liwei Guo: Supervision; Xiaonan Yang, Qiu Zhong , Xin Wu and Yi Wu: Project administration, Resources, Funding acquisition, Supervision, Visualization, Writing – review & editing.

REFERENCES

Alhobayb T and Ciorba MA, 2023. Clostridium difficile in inflammatory bowel disease. Curr. Opin. Gastroenterol 39:257–262. https://doi.org/10.1097/MOG.0000000000000949

Cai Y, Folkerts J, Folkerts G, *et al.,* 2020. Microbiota-dependent and -independent effects of dietary fibre on human health. Br J Pharmacol 177:1363–1381. https://doi.org/10.1111/bph.14871

Chen R, Xu J, Wu W, *et al.,* 2022. Structure-immunomodulatory activity relationships of dietary polysaccharides. Curr Res Food Sci 5:1330–1341. https://doi.org/10.1016/j.crfs.2022.08.016

Deng X, Huang J, Zhang M, *et al.,* 2023. Metabolite profiling and screening of callus browning-related genes in lotus (Nelumbo nucifera). Physiol. Plant 175:e14027. https://doi.org/10.1111/ppl.14027

Dilixiati Y, Aipire A, Song M, *et al.,* 2024. The Potential Role of Plant Polysaccharides in Treatment of Ulcerative Colitis. Pharmaceutics 16:1073. https://doi.org/10.3390/pharmaceutics16081073

Eisenstein M, 2018. Ulcerative colitis: towards remission. Nature 563:S33. https://doi.org/10.1038/d41586-018-07276-2

Fan Y and Pedersen O, 2021. Gut microbiota in human metabolic health and disease. Nat Rev Microbiol 19:55–71. https://doi.org/10.1038/s41579-020-0433-9

Feng J, Wang J, Bu T, *et al.,* 2023. Structural, in vitro digestion, and fermentation characteristics of lotus leaf flavonoids. Food Chem 406:135007. https://doi.org/10.1016/j.foodchem.2022.135007

Gurtner A, Borrelli C, Gonzalez-Perez I, *et al.,* 2023. Active eosinophils regulate host defence and immune responses in colitis. Nature 615:151–157. https://doi.org/10.1038/s41586-022-05628-7

Lin HV, Frassetto A, Kowalik EJ, *et al.,* 2012. Butyrate and propionate protect against diet-induced obesity and regulate gut hormones via free fatty acid receptor 3-independent mechanisms. PLoS One 7:e35240. https://doi.org/10.1371/journal.pone.0035240

Liu T, Asif IM, Liu L, *et al.,* 2024. Laminarin ameliorates iodoacetamide-induced functional dyspepsia via modulation of 5-HT (3) receptors and the gut microbiota. Int J Biol Macromol 268:131640. https://doi.org/10.1016/j.ijbiomac.2024.131640

Liu X, Zhang M, Chen S, *et al.,* 2024. Grifola frondosa polysaccharide's therapeutic potential in oxazolone-induced ulcerative colitis. Carbohydr Polym 344:122517. https://doi.org/10.1016/j.carbpol.2024.122517

Ma Z, Ma Y, Liu Y, *et al.,* 2023. Effects of Maturity and Processing on the Volatile Components, Phytochemical Profiles and Antioxidant Activity of Lotus (Nelumbo nucifera) Leaf. Foods 12:198. https://doi.org/10.3390/foods12010198

Ma Z, Zuo T, Frey N, *et al.,* 2024. A systematic framework for understanding the microbiome in human health and disease: from basic principles to clinical translation. Signal Transduct Target Ther 9:237. https://doi.org/10.1038/s41392-024-01946-6

Mukhopadhya I and Louis P, 2025. Gut microbiota-derived short-chain fatty acids and their role in human health and disease. Nat Rev Microbiol 23:635-651. https://doi.org/10.1038/s41579-025-01183-w

Peng Y, Zhu J, Li Y, *et al.,* 2024. Almond polysaccharides inhibit DSS-induced inflammatory response in ulcerative colitis mice through NF-kappab pathway. Int J Biol Macromol 281:136206. https://doi.org/10.1016/j.ijbiomac.2024.136206

Quaresma AB, Damiao A, Coy C, *et al.,* 2022. Temporal trends in the epidemiology of inflammatory bowel diseases in the public healthcare system in Brazil: A large population-based study. Lancet Reg. Health Am 13:100298. https://doi.org/10.1016/j.lana.2022.100298

Rees DC, Johnson E and Lewinson O, 2009. ABC transporters: the power to change. Nat Rev Mol Cell Biol 10, 218–227. https://doi.org/10.1038/nrm2646

Ruan Y, Zhu X, Shen J, *et al.,* 2024. Mechanism of Nicotiflorin in San-Ye-Qing rhizome for anti-inflammatory effect in ulcerative colitis. Phytomedicine 129:155564. https://doi.org/10.1016/j.phymed.2024.155564

Su Y, Huang J, Shi P, *et al.,* 2024. Lotus Leaf Extract Alleviates Lipopolysaccharide-Induced Intestinal Injury in Mice by Regulating Oxidative Stress and Inflammation. J Med Food 27:428–436. https://doi.org/10.1089/jmf.2023.K.0242

Tan Y, Cao W, Yang L, *et al.,* 2024. Structural characterization of the glucan from Gastrodia elata Blume and its ameliorative effect on DSS-induced colitis in mice. Int J Biol Macromol 275:133718. https://doi.org/10.1016/j.ijbiomac.2024.133718

Wang Z, Li Z, Wang H, *et al.,* 2024. Effects of Pine Pollen Polysaccharides and Sulfated Polysaccharides on Ulcerative Colitis in Mice by Regulating Th17/Treg. Foods 13:3183. https://doi.org/10.3390/foods13193183

Wei X, Wang F, Tan P, *et al.,* 2024. The interactions between traditional Chinese medicine and gut microbiota in cancers: Current status and future perspectives. Pharmacol Res 203:107148. https://doi.org/10.1016/j.phrs.2024.107148

Wu Y, Yin W, Hao P, et al 2024. Polysaccharide from panax japonicus c.a. Mey prevents non-alcoholic fatty liver disease development based on regulating liver metabolism and gut microbiota in mice. Int J Biol Macromol 260:129430. https://doi.org/10.1016/j.ijbiomac.2024.129430

Xu J, Tang C, Din AU, *et al.,* 2023. Oligosaccharides of Polygonatum Cyrtonema Hua ameliorates dextran sulfate sodium-induced colitis and regulates the gut microbiota. Biomed Pharmacother 161:114562. https://doi.org/10.1016/j.biopha.2023.114562

Yi L, Dong N, Yun Y *et al.,* 2016. Chemometric methods in data processing of mass spectrometry-based metabolomics: *A review.* Anal Chim Acta 914:17–34. https://doi.org/10.1016/j.aca.2016.02.001

Zhang Y, Lang R, Guo S *et al.,* 2022. Intestinal microbiota and melatonin in the treatment of secondary injury and complications after spinal cord injury. Front Neurosci 16:981772. https://doi.org/10.3389/fnins.2022.981772

Zhang Y, Ji W, Qin H, *et al.,* 2025. Astragalus polysaccharides alleviate DSS-induced ulcerative colitis in mice by restoring SCFA production and regulating th17/treg cell homeostasis in a microbiota-dependent manner. Carbohydr Polym 349:122829. https://doi.org/10.1016/j.carbpol.2024.122829

Zhao Y, Chen H, Li W, *et al.,* 2022. Selenium-containing tea polysaccharides ameliorate DSS-induced ulcerative colitis via enhancing the intestinal barrier and regulating the gut microbiota. Int J Biol Macromol 209:356-366. https://doi.org/10.1016/j.ijbiomac.2022.04.028

Zheng H, Han L, Shi W, *et al.,* 2022. Research Advances in Lotus Leaf as Chinese Dietary Herbal Medicine. Am J Chin Med 50:1423–1445. https://doi.org/10.1142/S0192415X22500616

Zhou R, He D, Xie J, *et al.,* 2021. The Synergistic Effects of Polysaccharides and Ginsenosides From American Ginseng (Panax quinquefolius L.) Ameliorating Cyclophosphamide-Induced Intestinal Immune Disorders and Gut Barrier Dysfunctions Based on Microbiome-Metabolomics Analysis. Front Immunol 12:665901. https://doi.org/10.3389/fimmu.2021.665901

Zhu X, Si F, Hao R, *et al.,* 2023. Nuciferine Protects against Obesity-Induced Nephrotoxicity through Its Hypolipidemic, Anti-Inflammatory, and Antioxidant Effects. J Agric Food Chem 71:18769–18779. https://doi.org/10.1021/acs.jafc.3c05735

Zioga N, Kogias D, Lampropoulou V, *et al.,* 2022. Inflammatory Bowel Disease-related Spondyloarthritis: The Last Unexplored Territory of Rheumatology. Mediterr J Rheumatol 33:126–136. https://doi.org/10.31138/mjr.33.1.126